AIAA JOURNAL
Vol. 54, No. 9, September 2016

Technical Notes

TECHNICAL NOTES are short manuscripts describing new developments or important results of a preliminary nature. These Notes should not exceed 2500 words (where a figure or table counts as 200 words). Following informal review by the Editors, they may be published within a few months of the date of receipt. Style requirements are the same as for regular contributions (see inside back cover).

Experimental Investigation on Transpiration Cooling Effectiveness for Spacecraft Entering Martian Atmosphere

S. Mohammed Ibrahim,* P. Vivek,† and K. P. J. Reddy‡
Indian Institute of Science, Bangalore 560 012, India

DOI: 10.2514/1.J054757

Nomenclature

H	=	enthalpy, MJ/kg
M	=	Mach number
P	=	pressure, kPa
R_b	=	base radius of the model, mm
R_n	=	nose radius of the model, mm
s	=	arc length on the model surface, mm
T	=	temperature, K
V	=	velocity, m/s
ρ	=	density, kg/m^3

Subscripts

o	=	reservoir conditions
∞	=	freestream conditions

I. Introduction

THE planet Mars has been a target for the space scientific community for the last four decades. The exploration of this planet was started in 17th century with the invention and development of telescopes. With the advancement in rocket technology, in the late 20th century, several missions to explore Mars were started. The first successful mission was Mariner 4, a flyby mission, to conduct scientific observation of the Martian environment and transmit the data back to Earth. Since then, several spacecraft has been sent to the planet for its exploration, which includes orbiters, landers, and rovers, with the recent ones being NASA's MAVEN and Indian Space Research Organization's MOM.

In the case of orbiters, the aerobraking technique can be used to position the spacecraft in required orbit (outer space) around the planet. However, for landers and rovers, the spacecraft have to pass through the atmosphere of the planet and reach its surface to start its mission. Martian atmospheric entry begins at an altitude of 125 km, and typical entry velocities vary from 4 to 9 km/s, depending on the entry trajectory [1]. At these entry speeds, the spacecraft are subjected to severe aerodynamic forces and aerodynamic heating, of which aerodynamic heating is a major aspect in the design of these spacecrafts.

Generally, large-angle blunt cones are used as forebodies for the spacecraft to minimize the aerodynamic heating [2–4]. These configurations also enhance aerodynamic drag, assisting in reducing the speed of the spacecraft during entry. However, the spacecraft requires an additional thermal protection system (TPS), acting as a barrier between the high-temperature gas in the shock layer and the spacecraft, during planetary entry. For any successful planetary entry, there is a need for an efficient thermal protection system.

The TPS used so far on all spacecraft entering Martian atmosphere is ablation cooling. In ablation cooling, the TPS material chars, melts, and undergoes pyrolysis, and the hot gas formed gets blown away, blocking the heat transfer to the surface. The material SLA-561V, superlightweight ablator, a proprietary material developed by Lockheed Martin, was used on all missions starting from Viking 1, except the Mars Science Laboratory (MSL) mission [5–8]. Phenolic impregnated carbon ablator, produced by Lockheed Martin and Fiber Materials Inc., was used for the MSL mission. The ablation cooling system, though successfully used in all missions to Mars, they have their own drawbacks.

1) During ablation, complex hydrocarbon products are formed, and their presence in the boundary layer of the spacecraft leads to a chemically reacting boundary layer, which can have an influence on aerodynamic forces and moments [9].

2) The shape change occurring during ablation can affect the aerodynamics of the spacecraft, resulting in change in flight path.

3) If the spacecraft experiences insufficient heat flux to cause pyrolysis, then the TPS will serve as thermal insulator rather than an ablator.

These drawbacks drove us to investigate the feasibility of using alternate TPS.

Over the years, several techniques like spiked forebodies as well as supersonic and sonic jet injection have been investigated for heat transfer rate reduction over atmospheric entry configurations [10–14]. Among these is transpiration cooling, a technique where the coolant gas from the plenum chamber is forced into the boundary layer of the spacecraft through a porous wall, as a result of which the coolant gas comes out as a continuous mass and forms a layer of it over the surface. A schematic of transpiration cooling is shown in Fig. 1.

The mechanism of transpiration cooling involves two steps. First, the coolant gas, on passing through the porous wall, absorbs the heat flux conducted into the material of the wall from the shock layer. Second, having passed through the porous wall, the coolant gas forms a film on the model surface, absorbs the heat flux partially through convection, and thus reduces the heat flux conducted into the wall from the high-temperature gas existing in the shock layer. The heated coolant gas is flushed downstream by the continuous supply of gas from the plenum chamber. In this way, the heat transferred to a vehicle traveling at hypervelocities can be greatly reduced. With the development of ceramic matrix composites like Carbon/Carbon ceramic, which can withstand very high temperatures and has natural porosity [15], transpiration cooling seems to be a promising technique. However, these materials have to be tested and validated for flight conditions encountered during planetary entry for application as TPS.

Received 1 October 2015; revision received 17 March 2016; accepted for publication 17 March 2016; published online 30 May 2016.

*Assistant Professor; currently National Institute of Technology, Kisarazu College, Japan.
†Research Scholar, Department of Civil Engineering, Karnataka.
‡Professor, Department of Aerospace Engineering, Karnataka.

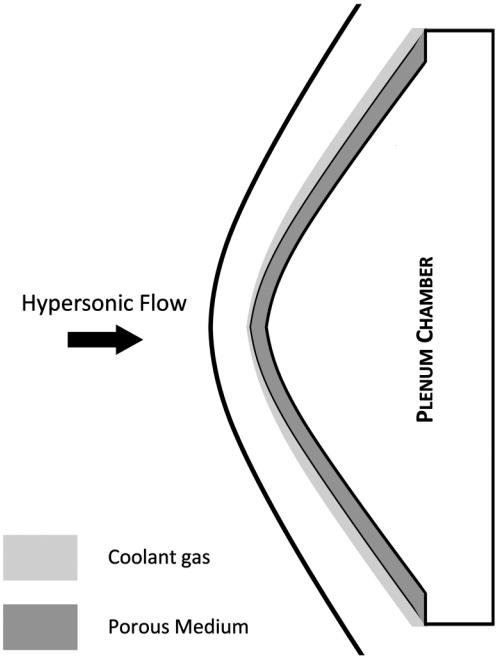

Fig. 1 Schematic of transpiration cooling.

Application of transpiration cooling at supersonic and hypersonic speeds has been investigated by several researchers and reported in the literature [16–20]. A review of this literature shows that the two important parameters that influence transpiration cooling are coolant gas mass flow rate and coolant gas specific heat capacity. Also, most of the transpiration cooling studies reported were carried out on geometries like flat plate, cone, and cylinder. Data for a realistic planetary entry configuration like large-angle blunt-cone forebodies were not available in the literature to the best of the authors' knowledge. Also, the reported studies were all carried out for Earth atmospheric entry. In this backdrop, an experimental campaign was started to investigate the effectiveness of transpiration cooling as TPS for Martian entry spacecraft. Because Martian atmosphere predominantly consists of carbon dioxide (95.32%) with small percentages of nitrogen (2.7%) and argon (1.6%) as well as traces of oxygen and carbon monoxide, we have used carbon dioxide as the test gas in the experiments reported here [21].

II. Experimental Facility

Experiments are carried out at flow enthalpies of 1.4 and 3.6 MJ/kg using hypersonic shock tunnels HST-2 and HST-3, respectively. HST-2 is a conventional shock-tunnel facility, operated in diaphragmless mode, consisting of driver and driven section separated using a direct acting solenoid valve ISTA KB-40. The driver side is filled with 40 bar of helium and driven with 0.22 bar of carbon dioxide (test gas). The fast opening of the valve results in the generation of a shock wave, which travels along the length of the driven section and, after its reflection at the end of the driven section, creates the reservoir condition for the nozzle. The nozzle and test section are initially maintained at vacuum level of 10^{-5} mbar using a rotary-diffusion pump and are separated from the driven side using a thin paper diaphragm. The test gas expands to hypersonic velocity in the nozzle and exits into the test section, where the test model is mounted, producing a steady flow test time of ~600 μs.

The HST-3 is a free-piston-driven facility, which is capable of simulating high-temperature or real gas effects. The facility consist of a high-pressure reservoir, compression tube in which the driver gas is compressed by a free piston running along its length, driven tube filled with test gas, convergent–divergent nozzle, test section, and dump tank. The reservoir is filled with 18 bar of nitrogen, which accelerates the 20 kg piston in the compression tube filled with 1 bar of helium, thereby compressing it to high pressure and temperature. The compression tube and driven tube are separated using aluminum diaphragm, which ruptures at a pressure of 93 $\pm$ 3 bar, resulting in the formation of a strong shock wave, which runs through driven tube filled with 0.22 bar of carbon dioxide. The shock wave after its reflection at the end wall creates the reservoir condition for the nozzle, which is separated initially using a thin paper diaphragm from the driven side. The test gas then expands to hypersonic speeds in the nozzle and flows steadily for a period of ~450 μs over the model mounted in the test section, which is maintained at vacuum level of 10^{-5} mbar using a rotary-diffusion pump assembly.

III. Test Model and Instrumentation

The test model used is a 60 deg apex angle blunt-cone forebody with nose radius of 35 mm and base radius of 40 mm. The forebody wall was made of plaster of Paris (POP), scientifically known as calcium sulphate hemihydrate, with 10 mm wall thickness and 40% porosity. POP was chosen as wall material because of its ease of preparation and cost effectiveness compared to sintered porous materials. A schematic view and photographic picture of the forebody and the model are shown in Figs. 2 and 3, respectively.

The heat transfer rates on the model surface are measured using platinum thin film sensors deposited on a Macor surface and flush mounted with the model. Four sensors were used, one in the nose region, one in the sphere–cone junction, and the remaining two in the conical region. An uncertainty analysis was carried out for heat transfer measurements based on the standard method given by Moffat [22]. The uncertainty depends on the errors in the output of the data-acquisition system including the error in reading the data from the signal ($\pm$3.15%), the thin-film gauge backing material property ($\pm$3.7%), the temperature coefficient of resistance of the platinum thin-film gauge ($\pm$2.5%), the measurement of initial voltage from the power supply ($\pm$1%), and the amplification factor in the measuring system ($\pm$1%). Thus, the uncertainty in the measured heat flux is estimated to be $\pm$5.65%.

The model gets the supply of coolant gas from an external high-pressure gas cylinder. The total supply pressure of the coolant gas was held at 6 $\pm$ 0.2 bar and was monitored using the pressure regulator. A pipe line from the supply cylinder connects to the flow meter, to

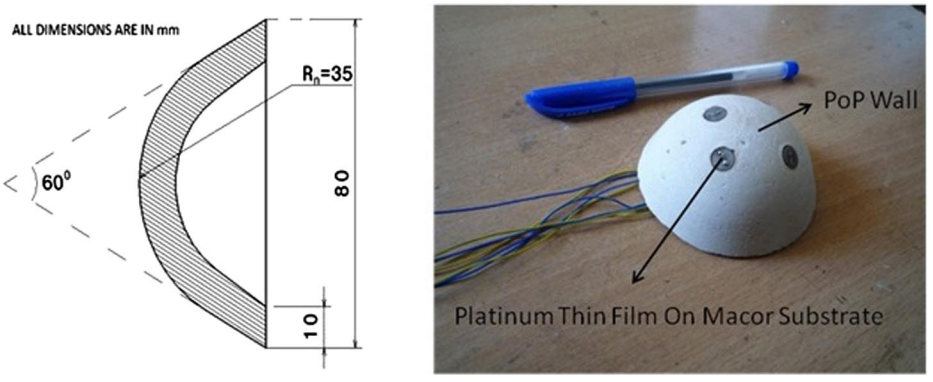

Fig. 2 Schematic and picture of 60 deg apex angle blunt-cone POP forebody.

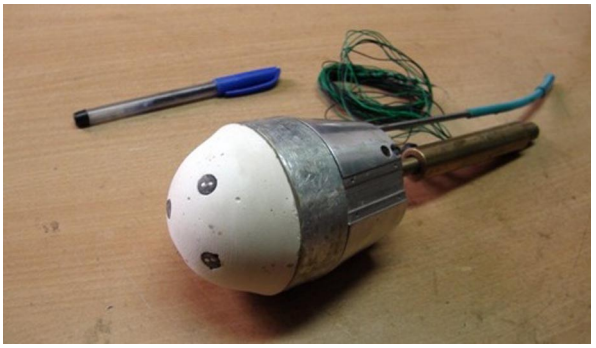

Fig. 3 Photographic picture of test model.

regulate the coolant gas mass flow rate, with an accuracy of ±5% of total range (0–500 l/ min). The output of the flow meter is connected to the test model mounted inside the test section.

IV. Experimental Results and Discussion

The effectiveness of transpiration cooling over a 60 deg blunt-cone forebody was investigated at two flow enthalpies, 1.4 MJ/kg (low enthalpy) and 3.6 MJ/kg (high enthalpy), in HST-2 and HST-3, respectively. The nozzle reservoir and freestream conditions generated for the two enthalpy cases are tabulated in Table 1. The nozzle reservoir conditions were calculated using the Chemkin reflected shock reactor assuming chemical and thermal equilibrium [23], and freestream properties were calculated assuming an isentropic nozzle expansion using corrected gamma and measured Pitot pressure [24]. The model was tested at 0 deg angle of attack in the presence and absence of transpiration cooling using nitrogen and helium gas as coolant.

A. Experiments at 1.4 MJ/kg

A total of four experiments were carried out for each case, and the mean values in heat transfer rates are taken and plotted. The shot-to-shot deviation in measured heat transfer rates was less than ±4 W/cm^2. The effect of coolant gas thermophysical properties and coolant gas mass flow rates on heat transfer distribution are explained next.

B. Influence of Coolant Gas

The effect of coolant gases, helium and nitrogen, on heat transfer rate distribution is plotted in Fig. 4 and in terms of Stanton number in Fig. 5. The supply mass flow rate was maintained the same, $2.6e^{-4}$ kg/s, for both coolants. In the absence of cooling, the heat transfer was higher in the nose region (stagnation zone) of the model and gradually decreased as we move downstream toward the conical region. With transpiration cooling, a reduction in heat transfer rate was observed on the model surface, and the trend in heat transfer distribution was preserved.

The percentage reduction in heat transfer due to transpiration cooling of helium and nitrogen gas is plotted in Fig. 6. In the nose region, the reduction in heat transfer was 25% and gradually increased to 41% in the conical region for helium, whereas for nitrogen coolant, it was 15% in the nose region and 22% in the conical region. This clearly shows that helium gas serves as a better coolant compared to nitrogen gas. This is due to the fact that the specific heat capacity of helium is higher (∼5 times) compared to nitrogen [16]; helium gas takes more heat from the shock layer compared to nitrogen. Also, for the same coolant gas mass flow rates, the volume flow rate and hence the velocity of helium gas diffusing out from the model surface are ∼7 times higher than nitrogen. This leads to a higher displacement of the boundary layer, hence an increase in its thickness and a lower temperature gradient across it, resulting in a larger reduction in heat transfer compared to nitrogen coolant gas. An increasing trend in percentage reduction in heat transfer was observed from the nose to the conical region of the test model. The surface pressure distribution imposed by the freestream flow will be higher in the nose region, being maximum at the stagnation point and gradually reducing toward the conical region of the model. This results in a higher blowing of coolant gas and hence higher percentage reduction in heat transfer rate with increasing distance from the stagnation point along the model surface.

Table 1 Properties in stagnation region and freestream for 1.4 and 3.6 MJ/kg

Properties	1.4 MJ/kg	3.6 MJ/kg
P_o, kPa	2797.08 ± 89.93	10233.5 ± 643
T_o, K	1246 ± 5.34	2877 ± 82
ρ_o, kg/m^3	12.74 ± 0.42	14.12 ± 0.24
M_∞	5.07 ± 0.02	5.87 ± 0.1
P_∞, kPa	1.06 ± 0.04	0.572 ± 0.055
T_∞, K	386.88 ± 2.87	739.85 ± 9
ρ_∞, kg/m^3	0.0145 ± 0.0004	0.0041 ± 0.0004
V_∞, m/s	1487.4 ± 1.65	2364.6 ± 12.35
Re_∞ million/m	1.13 ± 0.01	0.3 ± 0.01

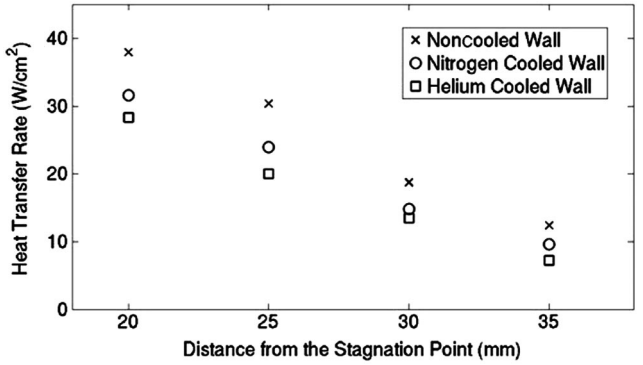

Fig. 4 Heat transfer rate distribution in the absence and presence of transpiration cooling at 1.4 MJ/kg.

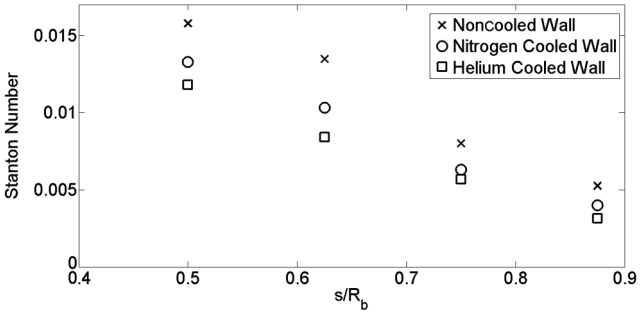

Fig. 5 Stanton number distribution in the absence and presence of transpiration cooling at 1.4 MJ/kg.

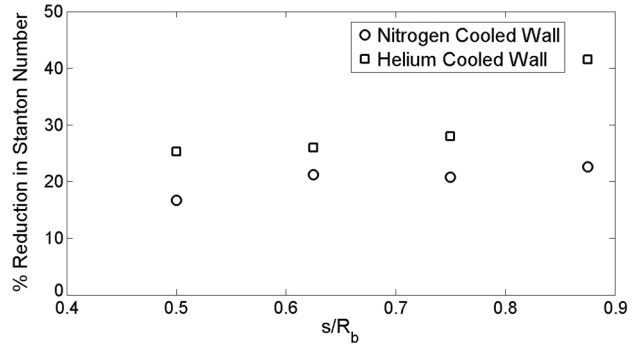

Fig. 6 Percentage reduction in Stanton number due to transpiration cooling at 1.4 MJ/kg.

C. Influence of Mass Flow Rate

The effects of coolant gas mass flow rate on heat transfer rate distribution on the model surface are plotted in terms of Stanton number in Fig. 7. Experiments were carried out using nitrogen gas as coolant at mass flow rates of $2.6e^{-4}$, $4.2e^{-4}$, and $6.4e^{-4}$ kg/s. A

reduction in heat transfer was observed with an increase in coolant mass flow rates. This reduction with increasing coolant mass flow was very significant in the nose region. However, as we move downstream toward the conical region, this was not the case. This is because, in the nose region (stagnation zone), the temperatures are higher, and more mass of coolant will take away more heat in the shock layer, whereas in the conical region, the temperatures are lower, and a little quantity of coolant gas will be sufficient to reduce the heat transfer.

D. Experiments at 3.6 MJ/kg

Experiments are carried out at high enthalpy to investigate the effectiveness of coolant gases used for transpiration cooling. The coolant gas mass flow rate was held the same $2.6e^{-4}$ kg/s for both nitrogen and helium coolant. A total of three experiments were carried out for each case, and the deviation in heat transfer measurements from shot to shot was less than ± 7 W/cm^2. The heat transfer rate and Stanton number distribution over the test model, in the absence and presence of transpiration cooling, are plotted in Figs. 8 and 9, respectively.

The trend in heat transfer distribution, in the absence of transpiration cooling, was similar to the 1.4 MJ/kg case. However, as expected, the heat transfer rates were significantly higher due to higher flow enthalpy. At higher flow enthalpy, high-temperature effects dominate the flowfield. The temperature in the shock layer is sufficient to cause vibrational excitation, dissociation, and recombination reaction of the test gas molecules [9]. A Chemkin analysis at 3.6 MJ/kg predicted dissociation of test gas molecules in the nozzle supply region [23]. The species formed, and their respective mole fractions are tabulated in Table 2. Chemkin analysis at 1.4 MJ/kg case did not predict any dissociation of test gas.

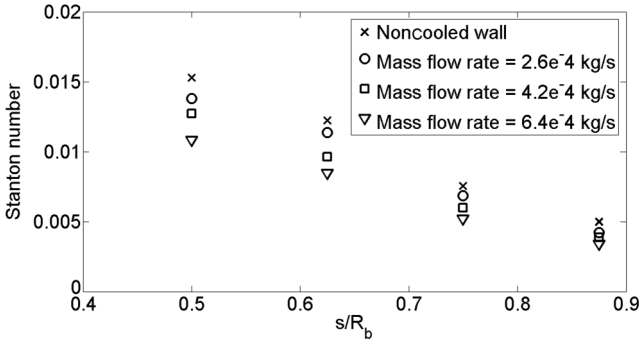

Fig. 7 Heat transfer rate distribution for varying coolant mass flow rate at 1.4 MJ/kg.

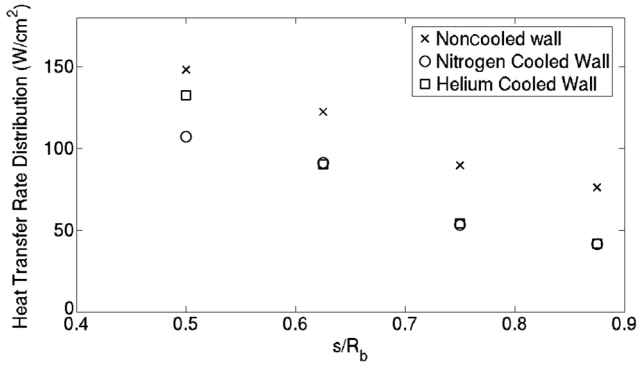

Fig. 8 Heat transfer rate distribution in the absence and presence of transpiration cooling at 3.6 MJ/kg.

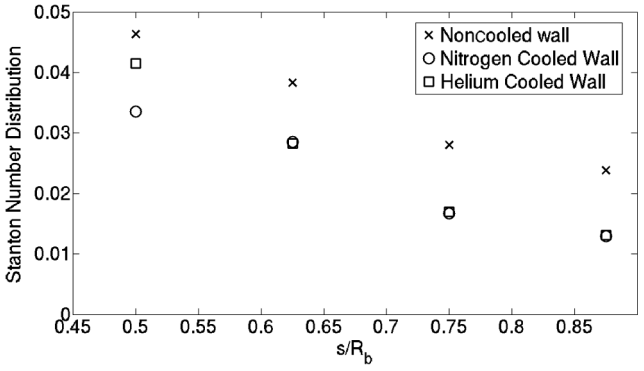

Fig. 9 Stanton number distribution in the absence and presence of transpiration cooling at 3.6 MJ/kg.

Table 2 Species and respective mole fraction at 3.6 MJ/kg

Species	Mole fraction
CO_2	0.889
CO	0.071
O_2	0.035
O	0.0012
C	$4.0e^{-13}$

In the presence of transpiration cooling, a reduction in heat transfer was observed for both nitrogen and helium coolant gas. The percentage reduction in heat transfer due to transpiration cooling for nitrogen and helium coolant is plotted in Fig. 10. Similar to the experiments at low enthalpy, an increasing trend in percentage reduction in heat transfer along the model surface was observed.

A higher reduction in heat transfer was observed when using nitrogen coolant. In the nose region of the model, at $s/R_b = 0.5$, the percentage reduction in heat transfer was 28% for nitrogen coolant, whereas for helium it was 10%. Along the conical portion of the test model, the percentage reductions for both coolants were almost the same. A completely different trend in heat transfer reduction was observed compared to the low-enthalpy case. Nitrogen coolant gas performed more effectively despite the fact that its heat capacity and volume flow rate are lower compared to helium gas, especially in the nose region of the model, where high-temperature effects are dominant. In the conical region of the model, the high-temperature effects will not be as significant as compared to the nose region; still, the effectiveness of nitrogen coolant in reducing the heat transfer rates was comparable to that of helium coolant. The better performance of nitrogen in the high-enthalpy case may be attributed to the diatomic nature of the gas, having translational, rotational, and Vibrational degrees of freedom to store energy. The temperature in the shock layer at 3.6 MJ/kg case is high enough to cause vibrational excitation and dissociation of nitrogen molecules diffusing out from the model surface.

A GASEQ analysis was carried out to check if there was any dissociation of injected nitrogen gas molecules at temperature of 2800 K, corresponding to freestream flow enthalpy of 3.6 MJ/kg, in the nose region of the model. The analysis was also carried out at temperatures ranging from 1500 to 2500 K, which would be the temperature range in the conical region of the model. The analysis involved both carbon dioxide test gas and injected nitrogen gas molecules in equal amount for all the temperature range, assuming chemical and thermal equilibrium. The predicted species and their respective mole fractions are tabulated in Table 3.

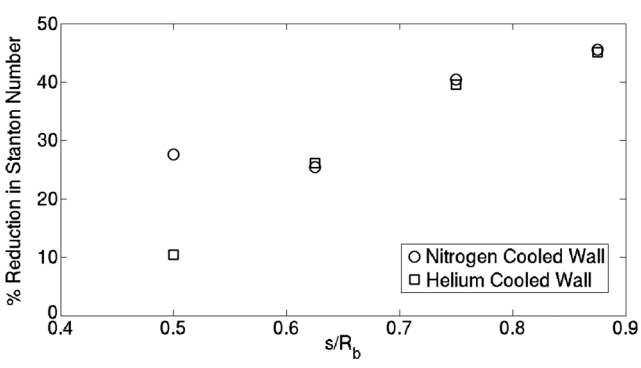

Fig. 10 Percentage reduction in Stanton number due to transpiration cooling at 3.6 MJ/kg.

Table 3 Species and respective mole fraction at temperature varying from 2800 to 1500 K

Species and mole fraction	At 2800 K	At 2500 K	At 2000 K	At 1500 K
CO_2	0.226	0.3613	0.4822	0.4946
CO	0.2135	0.1098	0.0142	$3.8e^{-4}$
O_2	0.0836	0.0476	0.0065	$1.6e^{-4}$
O	0.0284	0.0057	$9.7e^{-5}$	$9.3e^{-8}$
N_2	0.4306	0.4667	0.4959	0.4999
NO	0.0179	0.0089	0.0012	$3.0e^{-5}$

The analysis predicted dissociation of injected nitrogen gas molecules, with more dissociation in the nose region where temperatures are higher. The injected nitrogen molecules undergo significant vibrational excitation before dissociating. Both processes, vibrational excitation and dissociation, would have taken a fraction of the total amount of heat (energy) from the shock layer, resulting in a lower translational temperature, which is felt by the body as heat, whereas with helium coolant, being monoatomic and having only translational energy mode, the temperature of the injected coolant will be higher, resulting in a higher high heat transfer to the body than nitrogen coolant.

In the conical region of the model, dissociation of nitrogen gas molecules was not significant; however, it would have undergone significant vibrational excitation, resulting in a translational temperature similar to that of helium coolant. Hence, the performances of both coolants in reducing the heat transfer in the conical region of the test model were more or less the same.

V. Conclusions

An experimental study was carried out to investigate the effectiveness of the transpiration cooling technique, which can be used as TPS for spacecraft entering the Martian atmosphere. A 60 deg apex angle blunt-cone forebody was tested at flow enthalpies of 1.4 and 3.6 MJ/kg, both in the presence and absence of transpiration cooling. Two coolants were used, nitrogen and helium, and their effectiveness on heat transfer reduction was studied. The following are the conclusions drawn from the experiments.

1) In the presence of transpiration cooling, a reduction in heat transfer rates was observed for both flow enthalpies.

2) At low enthalpy, 1.4 MJ/kg, the use of helium gas as coolant resulted in a better heat transfer rate reduction than nitrogen gas, owing to its high specific heat capacity and larger volume flow rate.

3) An increase in heat transfer rate reduction was observed when increasing the coolant gas mass flow rate. This effect was more significant in the nose portion of the model, where the temperatures are higher than the conical portion.

4) At high enthalpy, 3.6 MJ/kg, nitrogen gas performed as a better coolant in the nose region of the test model. In the conical region, the performances of both coolants in reducing heat transfer rates were almost the same. This improved performance of nitrogen coolant gas, at high enthalpy flow, is attributed to the diatomic nature of the molecule, having additional energy modes to store energy, undergoing vibrational excitation and dissociation at higher temperatures.

Acknowledgments

We would like to thank the Defence Research and Development Organisation for the financial support as well as the members of the Laboratory for Hypersonic and Shock Wave Research for their support during the experiments.

References

[1] Tauber, M., Henline, W., Chargin, M., Papadopoulous, P., Chen, Y., Yang, L., and Hamm, K., "Mars Environmental Survey Probe Aerobrake Preliminary Design Study," *Journal of Spacecraft and Rockets*, Vol. 30, No. 4, 1993, pp. 431–437. doi:10.2514/3.25549

[2] Peter, F. I., and Donn, B. K., "High-Speed Aerodynamics of Several Blunt Cone Configurations," *Journal of Spacecraft and Rockets*, Vol. 24, No. 2, 1987, pp. 127–132.

[3] Stewart, D. A., and Chen, Y. K., "Hypersonic Convective Heat Transfer over 140-Deg Blunt Cones in Different Gases," *Journal of Spacecraft and Rockets*, Vol. 31, No. 5, 1994, pp. 735–743.

[4] Hollis, B. R., and John, N. P., "High-Enthalpy Aerothermodynamics of a Mars Entry Vehicle Part 1: Experimental Results," *Journal of Spacecraft and Rockets*, Vol. 34, No. 4, 1997, pp. 449–456.

[5] Congdon, W. M., "Ablation Model Validation and Analytical Sensitivity Study for the Mars Pathfinder Heat Shield," *30th Thermophysics Conference*, AIAA Paper 1995-2129, 1995.

[6] Szalai, C. E., Thoma, B. L., Lee, W. J., Maki, J. N., Willcockson, W. H., Venkatapathy, E., and White, T. R., "Mars Exploration Rover Heatshield Observation Campaign," *42nd AIAA Thermophysics Conference*, AIAA Paper 2011-3956, June 2011.

[7] McDaniel, R. D., Wright, M. J., and Songer, J. T., "Aeroheating Prediction for Phoenix Entry Vehicle," *46th AIAA Aerospace Sciences Meeting and Exhibit*, AIAA Paper 2008-1279, Jan. 2008.

[8] Bose, D., Santos, J. A., Erika, R., White, T., Olson, M., and Mahzari, M., "Mars Science Laboratory Heat Shield Instrumentation and Arc Jet Characterization," *44th AIAA Thermophysics Conference*, AIAA Paper 2013-2778, 2013.

[9] Anderson, J. D., *Hypersonics and High Temperature Gas Dynamics*, McGraw–Hill, New York, 1989, pp. 18–20.

[10] Stalder, J. R., and Nielsen, H. V., "Heat Transfer from a Hemisphere-Cylinder Equipped with Flow Separation Spikes," NACA TN-3287, 1954.

[11] Motoyama, N., Mihara, K., Miyajima, R., Watanuki, T., and Kubota, H., "Thermal Protection and Drag Reduction with Use of Spike in Hypersonic Flow," *10th AIAA/NAL-NASDA-ISAS International Space Planes and Hypersonic Systems and Technologies Conference*, AIAA Paper 2001-1828, April 2001.

[12] Romeo, D. J., and Sterrett, J. R., "Exploratory Investigation of the Effect of a Forward-Facing Jet on the Bow Shock of a Blunt Body in a Mach Number 6 Free Stream," NASA TN-D-1605, 1963.

[13] Barber, E. A., Jr., "An Experimental Investigation of Stagnation Point Injection," *Journal of Spacecraft and Rockets*, Vol. 2, No. 5, 1965, pp. 770–774. doi:10.2514/3.28277

[14] Sahoo, N., Kulkarni, V., Saravanan, S., Jagadeesh, G., and Reddy, K. P. J., "Film Cooling Effectiveness on a Large Angle Blunt Cone Flying at Hypersonic Speed," *Physics of Fluids*, Vol. 17, No. 3, 2005, Paper 036102. doi:10.1063/1.1862261

[15] Greuel, D., Herbertz, A., Haidn, O. J., Ortelt, M., and Hald, H., "Transpiration Cooling Applied to C/C Liners of Cryogenic Liquid Rocket Engines," *40th AIAA/ASME/SAE/ASEE Joint Propulsion Conference and Exhibit*, AIAA Paper 2004-3682, July 2004.

[16] Leo, T. C., and Howard, S. C., "Exploratory Test of Transpiration Cooling on a Porous 8 Degree Cone at $M = 2.05$ Using Nitrogen Gas, Helium Gas and Water as the Coolants," NACA RM-L55C29, 1955.

[17] Bernard, R., "Exploratory investigation of Transpiration Cooling of a 40° Double Wedge Using Nitrogen and Helium as Coolants at Stagnation Temperatures of 1295° to 2910° F," NACA RM-L57F11, 1957.

[18] Hirotaka, O., Fujita, K., and Ito, T., "Application of the transpiration Cooling Method for Reentry Vehicles," *45th AIAA Aerospace Sciences Meeting and Exhibit*, AIAA Paper 2007-1209, Jan. 2007.

[19] Esser, B., and Gülhan, A., "Qualification of Active Cooling Concepts in Ground Facilities," *RESPACE — Key Technologies for Reusable Space Systems*, Vol. 98, Notes on Numerical Fluid Mechanics and Multidisciplinary Design, Springer, 2008, pp. 104–131.

[20] Yuan, Q. L., Pei, X. J., Shao, S. J., and Ji, G. S., "Transpiration Cooling of a Nose Cone by Various Foreign Gases," *International Journal of Heat and Mass Transfer*, Vol. 53, Nos. 7–8, 2010, pp. 1260–1268. doi:10.1016/j.ijheatmasstransfer.2009.12.042

[21] Hepp, A. F., Landis, G. A., and Kubiak, C. P., "Chemical Approaches to Carbon Dioxide Utilization for Manned Mars Missions," NASA TM-103728, 1991.

[22] Moffat, R. J., "Describing the Uncertainties in Experimental Results," *Experimental Thermal and Fluid Sciences*, Vol. 1, No. 1, 1988, pp. 3–17.

[23] CHEMKIN, Software Package, Ver. 10113, Reaction Design, US, 2012, http://www.reationdesign.com/lobby/open/index.html [retrieved Feb. 2014]

[24] Ibrahim, S. M., and Reddy, K. P. J., "Heat Transfer Measurements over Large Angle Blunt Cones Entering Martian Atmosphere," *Journal of Spacecraft and Rockets*, Vol. 50, No. 3, 2013, pp. 719–722.

T. L. Jackson
Associate Editor